

# Motion Primitives for Human-Inspired Bipedal Robotic Locomotion: Walking and Stair Climbing

Matthew J. Powell, Huihua Zhao, and Aaron D. Ames

**Abstract**—This paper presents an approach to the development of bipedal robotic control techniques for multiple locomotion behaviors. Insight into the fundamental behaviors of human locomotion is obtained through the examination of experimental human data for walking on flat ground, upstairs and downstairs. Specifically, it is shown that certain outputs of the human, independent of locomotion terrain, can be characterized by a single function, termed the *extended canonical human function*. Optimized functions of this form are tracked via feedback linearization in simulations of a planar robotic biped walking on flat ground, upstairs and downstairs — these three modes of locomotion are termed “motion primitives.” A second optimization is presented, which yields controllers that evolve the robot from one motion primitive to another — these modes of locomotion are termed “motion transitions.” A final simulation is given, which shows the controlled evolution of a robotic biped as it transitions through each mode of locomotion over a pyramidal staircase.

## I. INTRODUCTION

The study of bipedal robotic locomotion has a rich history. An enormous variety of control approaches have been developed, including: passive walkers [1], [2], computation of zero-moment point [3] and clever use of compliance [4], among others. Robotic stair-climbing has been achieved in [5], [6]. Bipedal robots are even now available both commercially and for research. Impacts extend beyond the field with significant advances in prosthetic devices [7], [8], [9] and exoskeletons [10].

The quintessential model of bipedal locomotion — the human body — has an even richer history. Thousands of years of evolution has rendered the human locomotion system a highly effective, low-level control system. We suggest that examination of this system will yield unparalleled insight into the design of bipedal robotic locomotion controllers. Granted, the physical human system, which utilizes 57 muscles in locomotion [11], is far too complex to replicate with current hardware and computational capabilities; however, we claim that one can construct a low-level representation of the human locomotion system. That is, certain outputs of the human locomotion system can be represented as second order system responses.

This paper presents two main results; the first is an extension of [12], in which the author presents a method of automatically obtaining robotic walking controllers, via an optimization, from a set of human walking data. In the

present paper, it is shown that an augmentation of the optimization can be successfully applied to multiple modes of locomotion. Specifically, the presented technique yields robot locomotion controllers for walking on flat ground, upstairs and downstairs. The second result is a method of obtaining controllers which evolve the robot from one locomotion mode to another; that is, controllers which yield transition modes between walking on flat ground, and traversing stairs. The combination of these two results is a collection of controllers, automatically obtained from optimizations based on human data, which form a continuous, multi-modal system. Related to this work is the predictive simulation of human walking transitions method [13], which incorporates human motion capture data in an optimization to generate transition behaviors.

Here, the study begins with examination of the human locomotion system. Using the method of [12], it is shown that certain outputs of the human data for flat ground walking can be characterized by the response of a linear spring-damper system under constant force; this result is extended to accommodate walking upstairs and downstairs. Specifically, the *extended canonical human function* (3) is shown to represent sets of data, from all three modes of locomotion of interest, with high correlation in each case. The fact that the same function can be applied to different modes of locomotion further illustrates the validity of the proposed low-level representation of the human system.

A classification scheme for hybrid systems — the *meta-hybrid system* — is presented, in which a distinction is made between primary and auxiliary modes of locomotion, which are termed *motion primitives* and *motion transitions*, respectively. Motion primitives are fundamental modes of locomotion; the three motion primitives of this study are: walking on flat ground, walking upstairs and walking downstairs. To switch between different motion primitives, auxiliary modes, termed “motion transitions,” are introduced.

Implementing the extended canonical function via feedback linearization, stable locomotion is achieved on a planar bipedal robot in simulations of each of the three motion primitives. Motion transitions are used to construct simulations which show the composition of multiple motion primitives together; that is, a simulation is given which shows the controlled evolution of a biped as it ascends and then descends a staircase.

## II. HUMAN LOCOMOTION DATA

For guidance and insight in the control design process, we turn to the most prevalent source of information on bipedal

M. J. Powell, H. Zhao and A. D. Ames are with the Department of Mechanical Engineering, Texas A&M University, College Station, TX 77843, e-mail: {mjpowell, huihuazhao, aames}@tamu.edu

This research is supported by NASA grant NNX11AN06H, NSF grants CNS-0953823 and CNS-1136104, and NHARP award 00512-0184-2009.

walking found in nature — the human body. The following sections provide an overview of the analysis and the insights obtained through examination of the data.

**Human Locomotion Experiments.** A set of four human subjects participated in this study; each was outfitted with 19 LED sensors placed at key locations on the body,



Fig. 1: Human experiment for walking upstairs.

as illustrated in Fig. 1. As a test subject performed the desired task, data were collected from these sensors via the Phase Space Motion Capture System. An experiment consisted of a single test subject performing three distinct modes of locomotion: walking on flat ground, ascending a stairway and descending a stairway. The stairway used in this experiment has a 0.25 meter stair height and a 0.27 meter stair depth. For this paper, we selected the subject whose data contained the least noise; single steps from the data are determined via a domain breakdown procedure [14] — which entails the examination of heel position and acceleration data to determine instances of foot strike and foot lift.

**Extended Canonical Human Function.** In [15], it is shown that certain kinematic outputs of human walking can be represented by a single, universal function termed the “canonical human function” — which is the solution to a system of linear spring dampers under constant force. Examination of the data for walking up and down stairs, however, reveals a need for the augmentation of this function. It is found that both walking up and down stairs can be considered as the response of a spring-damper system to a constant force with sinusoidal excitation, which has the form

$$y = e^{-\zeta\omega_n t} (c_0 \cos(\omega_d t) + c_1 \sin(\omega_d t)) + g_0/\omega_n^2 + c_2(\omega_n, \omega, \zeta, b) \cos(\omega t) + c_3(\omega_n, \omega, \zeta, b) \sin(\omega t), \quad (1)$$

where  $c_0$  and  $c_1$  are the initial conditions decided by the initial position  $y(0)$  and the initial velocity  $\dot{y}(0)$ ;  $\xi$  is the damping ratio and  $\omega_n$  is the natural frequency;  $\omega_d = \sqrt{1 - \xi^2}\omega_n$  is the damped frequency; the constant term  $g_0$  is the gravity term;  $b$  and  $\omega$  are the amplitude and frequency of the sinusoidal excitation, respectively;  $c_2$  and  $c_3$  are functions of  $\omega_n$ ,  $\omega$ ,  $\xi$  and  $b$  given by:

$$\begin{aligned} c_2 &= (2b\xi\omega)/(\omega^4 + 2(-1 + 2\xi^2)\omega^2\omega_n^2 + \omega_n^4), \\ c_3 &= (b(-\omega^2 + \omega_n^2))/(\omega^4 + 2(-1 + 2\xi^2)\omega^2\omega_n^2 + \omega_n^4). \end{aligned} \quad (2)$$

Manipulation of (1) yields the following simplified form, which we term the *extended canonical human function*:

$$y_H(t) = e^{-\alpha_1 t} (\alpha_2 \cos(\alpha_3 t) + \alpha_4 \sin(\alpha_3 t)) + \alpha_5 \cos(\alpha_6 t) + \kappa(\alpha) \sin(\alpha_6 t) + \alpha_7, \quad (3)$$

where  $\kappa(\alpha) = (2\alpha_1\alpha_5\alpha_6)/(\alpha_1^2 + \alpha_3^2 - \alpha_6^2)$ .

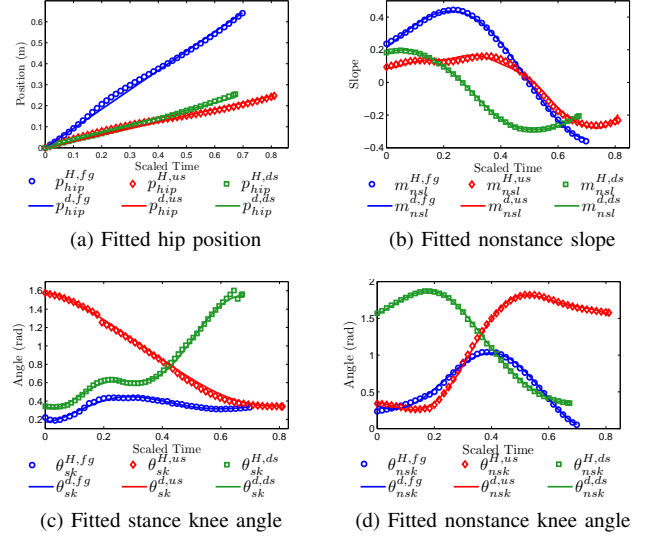


Fig. 2: Fitted extended canonical human functions and corresponding human data.

It will be shown that the extended canonical human function represents, with high correlation, certain outputs of human locomotion; this analysis forms the basis of the ideas and control approach presented in this paper. By examining outputs of human locomotion and showing that (3) fits these outputs with high correlation, we can construct a low-level representation of human locomotion. Through control, we can achieve locomotion — independent of terrain — which exhibits the same kinematic outputs of human locomotion in a robotic biped, despite immense morphological differences between human and robot.

**Function Fitting.** We now seek various kinematic properties, or constraints, of the human data which seem to describe the fundamental outputs of the human locomotion system. A total of four kinematic constraints are required for the 4-DOF robot model in consideration; the constraints chosen are: the forward position of the hip,  $p_{hip}$ , given by

$$p_{hip} = L_c \sin(-\theta_{sf}) + L_t \sin(-\theta_{sf} - \theta_{sk}),$$

where  $L_c$  and  $L_t$  are the lengths of the calf and thigh, respectively; the nonstance slope,  $m_{nsl}$ , given by

$$m_{nsl} = \frac{p_{nsl}^x - p_{hip}^x}{p_{nsl}^z - p_{hip}^z},$$

which defines the slope of a virtual line segment connecting the hip and the non-stance foot; the stance knee,  $\theta_{sk}$ ; and the non-stance knee,  $\theta_{nsk}$ . These constraints are illustrated on the robot model, in Fig. 3(c). Throughout the paper, the stance foot and nonstance foot are labeled  $sf$  and  $nsf$ , respectively.

Examination of human locomotion data reveals that the velocity of linearized hip position is approximately constant, as seen in Fig. 2(a). Thus, we fit the linearized hip position with straight line as  $\delta p_{hip}^d = \alpha_{v_{hip}} t$ . Utilizing the extended canonical function, the remaining three desired outputs of

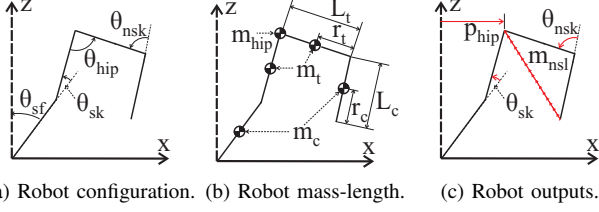


Fig. 3: The modeled robot’s configuration, mass & length distribution, and virtual constraints.

robot can be stated as:

$$\begin{aligned}
 \delta m_{nsl}^d(t, \alpha_{nsl}) &= y_H(t, \alpha_{nsl}), \\
 \theta_{sk}^d(t, \alpha_{sk}) &= y_H(t, \alpha_{sk}), \\
 \theta_{nsk}^d(t, \alpha_{nsk}) &= y_H(t, \alpha_{nsk}).
 \end{aligned} \quad (4)$$

where, e.g.,

$$\alpha_{sk} = (\alpha_{sk,1}, \alpha_{sk,2}, \alpha_{sk,3}, \alpha_{sk,4}, \alpha_{sk,5}, \alpha_{sk,6}, \alpha_{sk,7})$$

in (3). The parameters of all the outputs can be combined into a single parameter vector:  $\alpha = (\alpha_{vhip}, \alpha_{nsl}, \alpha_{sk}, \alpha_{nsk}) \in \mathbb{R}^{22}$ . By fitting these functions, via least square fits which yield high correlation coefficients, to corresponding human data, we claim that the canonical human function accurately describes human walking data. First, define the following human data-based cost function:

$$\text{Cost}_{\text{HD}}(\alpha) = \sum_{k=1}^K \sum_{i \in \text{Output}} (y_i^H[k] - y_i^d(t_i^H[k], \alpha_i))^2, \quad (5)$$

which is simply the sum of squared residuals; where  $i \in \text{Output} = \{\delta hip, \delta m_{nsl}, \theta_{sk}, \theta_{nsk}\}$ ;  $y_i^H[k]$  and  $y_i^d(\cdot)$  represent the mean human data and the canonical walking functions with fitting parameters  $\alpha_i$ , respectively, with  $k \in [1, \dots, K] \subset \mathbb{Z}$  an index for the  $K$  data points; for example,  $y_{\theta_{sk}}^H[k] = \theta_{sk}[k]$  and  $y_{\theta_{sk}}^d(t_{\theta_{sk}}^H[k], \alpha_{sk}) = \theta_{sk}^d(t_{\theta_{sk}}^H[k], \alpha_{sk})$ .  $t_i^H[k]$  is the discrete time for the mean human walking data.

To determine the parameters for the human walking functions, the following optimization is solved:

$$\alpha^* = \underset{\alpha \in \mathbb{R}^{22}}{\text{argmin}} \text{Cost}_{\text{HD}}(\alpha), \quad (6)$$

This optimization problem produces the least square fits of the canonical human functions to the corresponding human data (note that the reason this optimization is explicitly stated is because this same cost function will later be used, but subject to constraints that ensure robotic walking). The parameters obtained through this process are given in Table I, together with the correlation of each function to the corresponding set of data. Additionally, the functions for each kinematic constraint and each locomotion behavior (three motion primitives and four motion transitions) are plotted with the corresponding human data in Fig. 2.

### III. HYBRID AND META-HYBRID SYSTEMS

In this section, it is shown that primary modes of bipedal locomotion — such as walking, running, standing, jumping

and traversing stairways — can each be represented by a unique hybrid control system. However, control of functional bipedal robots requires dominion over *multiple* primary modes of locomotion. Therefore, to develop a functional locomotion control scheme, one must introduce auxiliary hybrid systems, which evolve the state of the robot during transitions between primary modes. To this end, we propose the concept of a meta-hybrid system, which consists of both primary and auxiliary hybrid systems.

#### A. Hybrid Systems

A natural choice of mathematical representation for this robot model is a hybrid system, or system with impulse effects [16], which exhibits both continuous and discrete dynamics.

*Definition 1:* A hybrid control system is a tuple,

$$\mathcal{HC} = (\mathcal{D}, S, \Delta, f, g, U),$$

where

- $\mathcal{D}$  is the domain with  $\mathcal{D} \subseteq \mathcal{X}$  a smooth submanifold of the state space  $\mathcal{X} \subseteq \mathbb{R}^n$ ,
- $S \subset \mathcal{D}$  is a proper subset of  $\mathcal{D}$  called the *guard* or *switching surface*,
- $\Delta : S \rightarrow \mathcal{D}$  is a smooth map called the *reset map*,
- $(f, g)$  is a *control system* on  $\mathcal{D}$ , i.e.,  $\dot{x} = f(x) + g(x)u$ ,
- $U \subseteq \mathbb{R}^m$  is the set of admissible control.

A *hybrid system* is a hybrid control system with  $U = \emptyset$ , e.g., any applicable feedback controllers have been applied, making the system closed-loop. In this case,

$$\mathcal{H} = (\mathcal{D}, S, \Delta, f),$$

where  $f$  is a dynamical system on  $\mathcal{D} \subseteq \mathcal{X}$ , i.e.,  $\dot{x} = f(x)$ .

**Hybrid System for the Biped.** The robot model for this work is a planar, four-link pinned kinematic chain, with a configuration and mass and length distribution as shown in Fig. 3(a) and 3(b), in which  $m_c, m_t, m_{hip}$  are the masses of the calf, thigh and hip, respectively;  $L_c$  and  $L_t$  are the lengths of the calf and thigh;  $r_c$  and  $r_t$  are the locations of the center of mass of the calf and thigh, as measured from the foot and knee. Derivations of the Lagrangian dynamics and impact model for this biped are given in detail in [12].

TABLE I: Fitted parameter values for human functions.

f.	$y_1^d = a_1 t, \quad y_2^d = y_H(t)$ given in (3)							Corr.
	$a_1$	$a_2$	$a_3$	$a_4$	$a_5$	$a_6$	$a_7$	
$p_{hip}^{fg}$	0.921	0	0	0	0	0	0	0.9982
$p_{hip}^{us}$	0.273	0	0	0	0	0	0	0.9954
$p_{hip}^{ds}$	0.357	0	0	0	0	0	0	0.9976
$m_{nsl}^{fg}$	-1.135	0.062	6.495	0.217	0	0	0.150	0.9995
$m_{nsl}^{us}$	-0.515	0.057	5.515	0.162	0.046	14.864	-0.017	0.9996
$m_{nsl}^{ds}$	0.475	0.242	6.937	0.149	0.008	23.294	-0.076	0.9999
$\theta_{sk}^{fg}$	2.475	-0.188	10.248	-0.011	0	0	0.358	0.9861
$\theta_{sk}^{us}$	2.013	1.028	3.705	0.639	0.023	14.375	0.514	0.9994
$\theta_{sk}^{ds}$	1.775	-2.383	0.6909	-8.130	-0.130	11.374	2.852	0.9390
$\theta_{nsk}^{fg}$	-0.849	-0.288	9.131	-0.123	0	0	0.593	0.9976
$\theta_{nsk}^{us}$	0.089	-0.850	5.367	-0.161	0.157	14.268	1.046	0.9996
$\theta_{nsk}^{ds}$	-1.222	0.330	6.266	0.312	-0.066	15.422	1.289	0.9999

Given the preceding definition, we can now build a hybrid system representation of the robot model of this study. Formally, we begin by writing the hybrid control system for the robot as:

$$\mathcal{H}\mathcal{C}_h^R = (\mathcal{D}_h^R, S_h^R, \Delta^R, f^R, g^R, U^R), \quad (7)$$

which depends on a unilateral constraint function,  $h$ , that represents the environment, or *terrain* of the hybrid system. Specifically,  $h$  is the height of non-stance foot above the walking surface, e.g., a staircase or flat ground;  $h$  characterizes the allowable configuration, i.e. the domain, given by:

$$\mathcal{D}_h^R = \{(q, \dot{q}) \in T\mathcal{Q} : h(q) \geq 0\}. \quad (8)$$

The guard is just the boundary of the domain with the additional assumption that the unilateral constraint is decreasing, i.e., the vector field is pointed outside of the domain, or

$$S_h^R = \left\{ (q, \dot{q}) \in T\mathcal{Q} : h(q) = 0 \text{ and } \frac{\partial h(q)}{\partial q} \dot{q} < 0 \right\}. \quad (9)$$

The remaining elements are specified by the dynamics of the robot; that is, they are intrinsic to the model and consistent for all hybrid system representations of the robot, yet they are independent of the terrain. These elements are given by

- $\Delta^R$  is the reset map — corresponding to the equations which describe the response of the system to foot-ground impact. Here the impact model of [17] is employed, which assumes perfectly plastic impacts.
- $(f^R, g^R)$  is a *control system* on  $\mathcal{D}^R$  — which governs the evolution of the continuous phase of bipedal locomotion. The Euler-Lagrange equations, (see [18]), are used to obtain the control system for a given biped model.
- $U^R = \mathbb{R}^4$ , as we assume full control authority.

**Controller Design.** Motivated by the desire to obtain human-like, bipedal robotic locomotion, we seek to construct a controller which drives outputs of the robot to corresponding outputs of the human. Formally, we seek a  $u$  which guarantees that  $y^a(q) \rightarrow y^d(t)$  as  $t \rightarrow 0$ , where  $q$  is the configuration space of the biped,  $y^a$  is the actual value of the constraint on the robot and  $y^d$  is the value of the extended canonical human function. As the dynamics of the robot model are highly nonlinear, the natural choice of control method for this system is Input/Output Linearization [19].

The construction of this control law uses the human walking functions considered in Sect. II. With these functions in mind, we define the (relative degree 2) actual outputs of the robot to be the output functions considered in Sect. II and the desired outputs to be the outputs of the human as represented by the walking functions:

$$y_2^a(q) = \begin{bmatrix} m_{nsl}(q) \\ \theta_{sk} \\ \theta_{nsk} \end{bmatrix}, \quad y_{2,\alpha}^d(t) = \begin{bmatrix} m_{nsl}^d(t, \alpha_{nsl}) \\ \theta_{sk}^d(t, \alpha_{sk}) \\ \theta_{nsk}^d(t, \alpha_{nsk}) \end{bmatrix}. \quad (10)$$

Similarly, with the goal of controlling the velocity of the robot, we define the relative degree 1 outputs to be the

velocity of the hip and the desired velocity of the hip:

$$y_1^a(q, \dot{q}) = dp_{\text{hip}}(q)\dot{q}, \quad y_{1,\alpha}^d = v_{\text{hip}}. \quad (11)$$

The goal is for the outputs of the robot to agree with the outputs of the human, motivating the final form of the outputs to be used in feedback linearization:

$$y_{1,\alpha}(q, \dot{q}) = y_1^a(q, \dot{q}) - v_{\text{hip}}, \quad (12)$$

$$y_{2,\alpha}(q) = y_2^a(q) - y_{2,\alpha}^d(\tau(q)) \quad (13)$$

where  $\tau(q)$  is a state-based parameterization of time using the forward position of the hip; this renders the control system autonomous. The controller  $u$  is obtained via feedback linearization with the human-inspired virtual outputs (12) and (13). A full derivation of the control law is given in [12], but we note that the feedback linearization controller depends on a constant  $\epsilon$  which controls the convergence to the zero dynamics surface, with faster convergence as  $\epsilon \rightarrow \infty$ .

For the hybrid control system  $\mathcal{H}\mathcal{C}_{h,\alpha}^R$ , we apply the human-inspired control law to obtain a hybrid system:

$$\mathcal{H}_{(h,\alpha)}^R = (\mathcal{D}_{(h,\alpha)}^R, S_{(h,\alpha)}^R, \Delta^R, f_\alpha^R), \quad (14)$$

with

$$f_\alpha^R(q, \dot{q}) = f^R(q, \dot{q}) + g^R(q, \dot{q})u_\alpha(q, \dot{q}).$$

Here, we have made the dependence of  $f_\alpha^R$  on the parameters  $\alpha \in \mathbb{R}^{22}$  of the human walking functions explicit (note that  $f_\alpha^R$  also depends on the control gain  $\epsilon$ , but since the same gain will be used in all cases for the robot it is not explicitly stated). The end result of the modeling process is a hybrid system  $\mathcal{H}_{h,\alpha}^R$  that depends on both the terrain (through  $h$ ) and the parameters of the human inspired control  $\alpha$ .

## B. Meta-Hybrid Systems.

A meta-hybrid system is a hybrid system of hybrid systems, which contains multiple locomotion behaviors and transitions between these behaviors.

*Definition 2:* A *meta-hybrid system* is a tuple,

$$\mathcal{M}\mathcal{H} = (\Gamma, \mathcal{M}, \mathcal{T})$$

where

- $\Gamma = (V, E)$  is a directed graph, with  $V$  a set of vertices, or nodes, and  $E \subset Q \times Q$  a set of edges; for  $e = (q, q') \in E$ , denote the source of  $e$  by  $\text{sor}(e) = q$  and the target of  $e$  by  $\text{tar}(e) = q'$ .
- $\{\mathcal{M}_v\}_{v \in V}$  is a collection of *motion primitives*, each represented by a hybrid system:

$$\mathcal{M}_v = (\mathcal{D}_v, S_v, \Delta_v, f_v, U_v).$$

- $\{\mathcal{T}_e\}_{e \in E}$  is a collection of *motion transitions*, represented by hybrid systems of the form:

$$\mathcal{T}_e = (\mathcal{D}_{\text{tar}(e)}, S_{\text{tar}(e)}, \Delta_{\text{tar}(e)}, f_e).$$

That is,  $\mathcal{T}_e$  has the same domain, guard and reset map as  $\mathcal{M}_{\text{tar}(e)}$ , but has a different vector field  $f_e$ .

It is important to note that the meta-hybrid system of a hybrid system, except that we have placed explicit restrictions on the structure of this system so as to be applicable

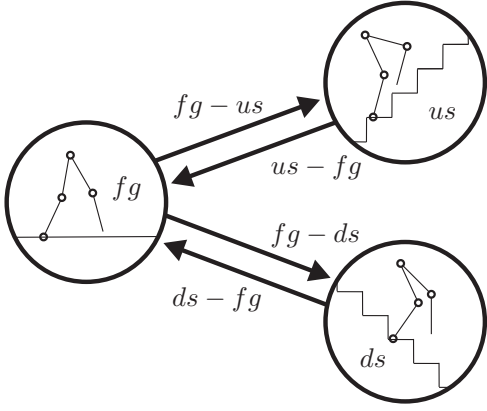


Fig. 4: Graph of a meta-system representation for the three motion primitives in consideration.

to bipedal robots that switch between different walking behavior. In particular, as will be seen, we will construct three motion primitives and transitions behaviors to form a meta-hybrid system as illustrated in Fig. 4.

#### IV. MOTION PRIMITIVES & TRANSITIONS

In this section, we will explicitly construct a meta-hybrid system for a bipedal robot, with the motion primitives—walking on flat ground, walking upstairs and walking downstairs—and transitions between these behaviors. The behavior of the robot performing these transitions and motion primitives will be supported through simulation results. More formally, the goal of this section is to construct a meta-hybrid system for the bipedal robot:

$$\mathcal{MH}^R = (\Gamma^R, \mathcal{M}^R, \mathcal{T}^R).$$

Since the three motion primitives we are interested in are walking on flat ground, walking up stairs, and walking down stairs, we have the directed graph  $\Gamma^R = (V^R, E^R)$ , where

$$\begin{aligned} V^R &= \{fg, us, ds\} \\ E^R &= \{(fg, us), (us, fg), (fg, ds), (ds, fg)\} \end{aligned}$$

or we allow transitions between walking on flat ground and going up and down stairs (but not transitions between going up stairs and going down stairs). The graph  $\Gamma^R$  can be seen in Fig. 4. The remainder of this section will be devoted to constructing the motion primitives and motion transitions.

##### A. Motion Primitives

Motion primitives are the core modes of locomotion of this study; this section discusses the development of controllers for motion primitives and the simulations resulting from the application of these controllers to the robot model.

**Motion Primitive Collection.** Using the concepts developed throughout this paper, and specifically Sect. III-A, we can now construct mathematical representations of a bipedal robot traversing each of the three different terrains of interest: walking on flat ground  $fg$ , up stairs  $us$ , and down stairs  $ds$ . In particular, for each of the three terrains we obtain a hybrid

system (of the form given (14)) modeling the biped in this terrain:

- *Flat Ground:*  $\mathcal{H}_{(h_{fg}, \alpha_{fg})}^R$ , where  $h_{fg}(q) = p_{nsf}^z(q)$  is the height of the foot above flat ground,
- *Up Stairs:*  $\mathcal{H}_{(h_{us}, \alpha_{us})}^R$ , where  $h_{us}(q) = p_{nsf}^z(q) - p_{stair}^z$  is the height of the foot above a stair (with the stair above the stance foot).
- *Down Stairs:*  $\mathcal{H}_{(h_{ds}, \alpha_{ds})}^R$ , where  $h_{ds}(q) = p_{nsf}^z(q) + p_{stair}^z$  is the height of the foot above a stair (with the stair below the stance foot).

To achieve motion primitives from these hybrid systems, it is necessary to design controllers for each motion primitive, i.e., determine the control parameters  $\alpha_v, v \in V^R$ , that will result in stable walking for the robot in each terrain.

**Controller Development.** To obtain the control parameters  $\alpha_v, v \in V^R$ , for each motion primitive, we use the method of [12] which uses human data in the form of an optimization subject to constraints that imply stable walking (see [20] for the underactuated case). In particular, we solve the optimization problem:

$$\begin{aligned} \alpha_v^* &= \underset{\alpha_v \in \mathbb{R}^{22}}{\operatorname{argmin}} \operatorname{Cost}_{\text{HD}}(\alpha_v) \\ \text{s.t. } &\Delta^R(S_{h_v}^R \cap \mathbf{Z}_{\alpha_v}) \subset \mathbf{PZ}_{\alpha_v} \end{aligned} \quad (15)$$

where  $\operatorname{Cost}_{\text{HD}}$  is the human-data-based cost function, (5); note that since this cost depends on the human data, it is indexed by  $v \in V^R$  since for each motion primitive one obtains a different cost. Moreover, the constraints of the optimization depend on the constraint function  $h_v, v \in V^R$ , i.e., they depend on the specific terrain being considered. Finally,  $\mathbf{Z}_{\alpha_v}$  is a *zero dynamics surface* of the system, on which  $y_1^a(q, \dot{q}) = y_{1, \alpha_v}^d$  and  $y_2^a(q) = y_{2, \alpha_v}^d(q)$  for all time;  $\mathbf{PZ}_{\alpha_v}$  is a *partial zero dynamics surface* of the system, on which  $y_2^a(q) = y_{2, \alpha_v}^d(q)$  for all time. Due to space constraints, we refer the reader to [12] for further details.

By solving the optimization problem (15) for each motion primitive, we obtain control parameters  $\alpha_v^*, v \in V^R$  that yield stable hybrid systems for each motion primitive (this is formally proven in [21] and will be justified through simulation in the next paragraph). Moreover, a fixed point for each motion primitive  $(q_v^*, \dot{q}_v^*) \in S_{h_v}^R, v \in V^R$ , i.e., the unique point on the periodic orbit that intersects the guard, can be computed in closed form in the limit as  $\epsilon \rightarrow \infty$  (again see [21]). That is, we have thus obtained the motion primitives for  $\mathcal{MH}^R$  given by  $\mathcal{M}_v^R = \mathcal{H}_{(v, \alpha_{h_v}^*)}^R, v \in V^R$ . Plots of the human walking functions with the specific parameters  $\alpha_v^*$  found by solving this optimization problem, as compared against the human data, can be seen in Fig. 5. By inspecting that figure, it can be seen that the canonical human walking functions that yield walking for each motion primitive have very good agreement with the human walking data.

**Simulations.** A simulation for each motion primitive was performed. The resulting locomotion gaits from simulation are given in Fig. 7; these figures show the evolution of the robot during the single support phase of the gait, each of

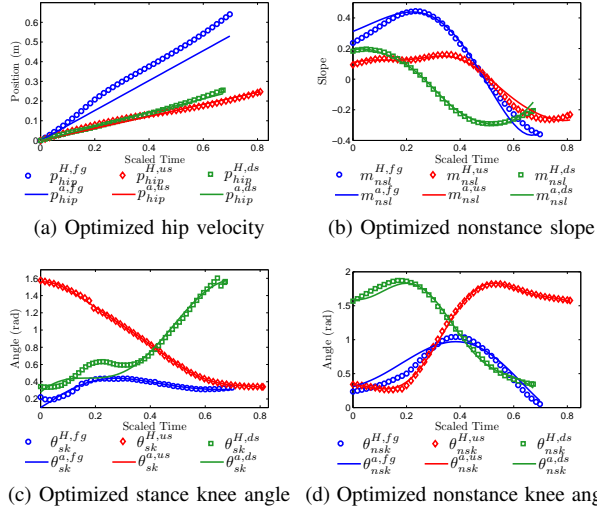


Fig. 5: Optimized extended canonical human functions with parameters obtained by solving the optimization problem (15) and the corresponding human data.

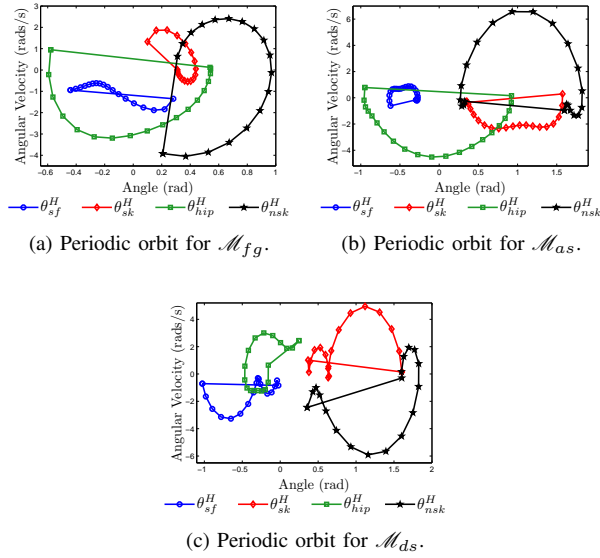


Fig. 6: Phase portraits for the motion primitives.

which qualitatively resembles the corresponding human gait quite well. The phase portraits for each motion primitive simulation are shown in Fig 6. Numerical approximations of the Poincaré map yield eigenvalues with magnitude less than one, implying that the corresponding motion primitives are stable.

### B. Motion Transitions

This section discusses the development and simulation of motion transitions which are explicitly built upon the motion primitives obtained in the previous section.

**Motion Transition Collection.** We are interested in developing motion primitives based upon the meta-hybrid system graph  $\Gamma^R$ , which gives the allowable transitions between

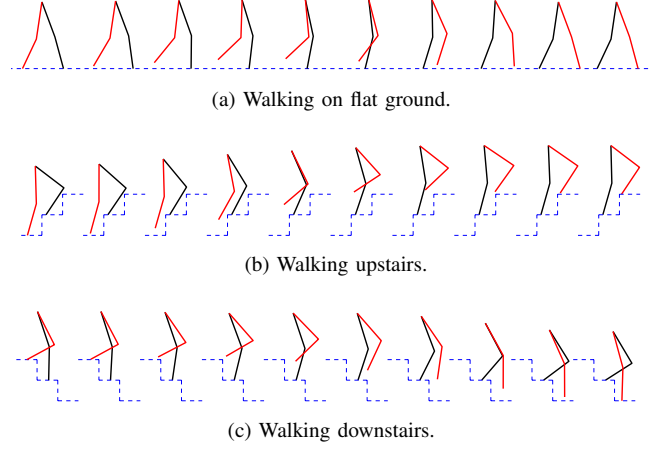


Fig. 7: Snapshots from robotic locomotion simulations exhibiting the three motion primitives. The stance leg is shown in black; the nonstance leg is shown in red.

different walking behaviors. Based upon the definition of a meta-hybrid system (Definition 2), the motion transitions must satisfy very specific conditions with regard to the motion primitives. Therefore, specific motion transition hybrid systems we are interested in must have the form:

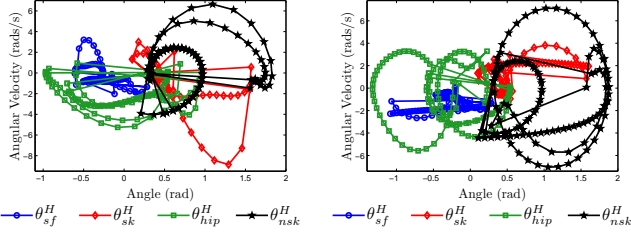
- Walking on flat ground to up stairs:  $\mathcal{H}_{(h_{us}, \alpha_{(fg, us)})}^R$
- Walking up stairs to flat ground:  $\mathcal{H}_{(h_{fg}, \alpha_{(us, fg)})}^R$
- Walking on flat ground to down stairs:  $\mathcal{H}_{(h_{ds}, \alpha_{(fg, ds)})}^R$
- Walking down stairs to flat ground:  $\mathcal{H}_{(h_{fg}, \alpha_{(ds, fg)})}^R$

Therefore, to define the transition behaviors, it is necessary to determine the control parameters  $\alpha_e$ ,  $e \in E$ . This will be achieved through another optimization, but one that uses the walking behavior of the motion primitives to smoothly transition from one behavior to another.

**Controller Development.** To determine the parameters  $\alpha_e$ ,  $e \in E$ , of the motion transitions we use the fixed points corresponding to the stable walking of each motion primitive. In particular, let  $(q_v^*, \dot{q}_v^*) \in S_{h_v}^R$ ,  $v \in V^R$ , be the fixed point of each motion primitive obtained through (15). Using this, and at a high level, the goal of the motion transition optimization is to generate desired output functions, which have smooth connections with the corresponding source and the target motion primitives. Formally, these objectives can be stated in an optimization problem:

$$\begin{aligned} \alpha_e^* &= \underset{\alpha \in \mathbb{R}^{22}}{\operatorname{argmin}} \quad \dot{y}_{2, \alpha_e}^d(\tau_{\alpha_e}) - \dot{y}_{2, \alpha_{\operatorname{tar}(e)}^*}^d(\tau_{\alpha_{\operatorname{tar}(e)}^*}(q_{\operatorname{tar}(e)}^*)) \quad (16) \\ \text{s.t.} \quad & y_{2, \alpha_e}^d(0) - y_{2, \alpha_{\operatorname{sor}(e)}^*}^d(0) = 0 \\ & \dot{y}_{2, \alpha_e}^d(0) - \dot{y}_{2, \alpha_{\operatorname{sor}(e)}^*}^d(0) = 0 \\ & y_{2, \alpha_e}^d(\tau_{\alpha_e}) - y_{2, \alpha_{\operatorname{tar}(e)}^*}^d(\tau_{\alpha_{\operatorname{tar}(e)}^*}(q_{\operatorname{tar}(e)}^*)) = 0 \\ & y_{1, \alpha_e}^d - \frac{y_{1, \alpha_{\operatorname{sor}(e)}^*}^d + y_{1, \alpha_{\operatorname{tar}(e)}^*}^d}{2} = 0 \end{aligned}$$

where  $\tau_{\alpha_{\operatorname{tar}(e)}^*}$  is the parameterization of time based upon the position of the hip (see [12]), and  $\tau_{\alpha_e}$  is a parameterization



(a) Periodic orbit for  $\mathcal{H.M.}_{\{fg,us\}}$ . (b) Periodic orbit for  $\mathcal{H.M.}_{\{fg,ds\}}$ .  
 Fig. 8: Phase portraits for the motion primitive-transition combinations.

of time for the motion transition,  $\tau_{\alpha_e} = (p_{hip}(q_{target}^*) - p_{hip}(\Delta^R(q_{source}^*))) / v_{hip}$ ,  $y_{2,\alpha_e}^d(t)$  is the desired output of the robot with parameters  $\alpha_e$ ;  $\alpha_{tar(e)}^*$  and  $\alpha_{sor(e)}^*$  are the parameters of the target and source motion primitives,  $\mathcal{M}_{tar(e)}^R$  and  $\mathcal{M}_{sor(e)}^R$ , respectively. They are obtained by solving the optimization problem (15),  $(q_{tar(e)}^*, \dot{q}_{tar(e)}^*)$  is the fixed point of the periodic orbit for the target motion primitive. Solving this optimization problem yields parameters  $\alpha_e^*$ ,  $e \in E^R$ , which yields our motion transition hybrid systems:  $\mathcal{T}_e = \mathcal{H}_{(h_{tar(e)}, \alpha_e^*)}^R$  with  $e \in E^R$ .

**Simulations.** Three simulations were performed in which motion primitives and motion transitions were combined. To construct a Poincaré map, and thus establish a notion of the stability of a meta-system, the biped must start and end in the same mode; therefore, we chose to simulate two locomotion cycles: walking on flat ground to walking up stairs to walking on flat ground (F-US-F) and walking on flat ground to walking down stairs to walking on flat ground (F-DS-F). The phase portrait for each locomotion cycle is shown in Fig. 8. Numerical approximation yields eigenvalues for both simulations; the maximum eigenvalue of each is below unity which implies that both meta-systems are stable. Finally, we simulated all three motion primitives together with the four motion transitions; see Fig. 9 for snapshots from the simulated walking gait.

## V. CONCLUDING REMARKS

In this paper, we examined experimental human data on three modes of walking. It is shown that certain outputs of the flat ground *and* stair-climbing data can each be represented by the response of a linear spring-damper system. An optimization of the parameters in (3) gives virtual outputs for feedback linearization controllers; implementation of these controllers yields stable, periodic locomotion in simulation. A second optimization yields controllers which effect transitions between motion primitives; these intermediate modes are termed *motion transitions*. Simulations are given which display bipedal robots walking in a varying terrain. Future work will be devoted to expanding the set of motion primitives to additional locomotion behaviors, extending the results presented to the case of underactuation, and finally realizing the results of this work on a physical robot.

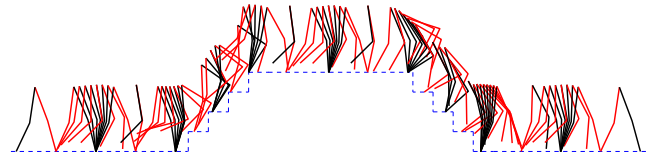


Fig. 9: Snapshots from the simulated composition of multiple locomotion modes. The stance leg is shown in black; the nonstance leg is shown in red.

## REFERENCES

- [1] S. Collins, A. Ruina, R. Tedrake, and M. Wisse, "Efficient bipedal robots based on passive-dynamic walkers," *Science*, vol. 307, pp. 1082–1085, Feb. 2005.
- [2] M. W. Spong and F. Bullo, "Controlled symmetries and passive walking," *IEEE TAC*, vol. 50, no. 7, pp. 1025–1031, 2005.
- [3] C. Chevallereau, D. Djoudi, and J. W. Grizzle, "Stable bipedal walking with foot rotation through direct regulation of the zero moment point," *IEEE TRO*, vol. 25, no. 2, pp. 390–401, Apr. 2008.
- [4] J. Pratt, P. Dilworth, and G. Pratt, "Virtual model control of a bipedal walking robot," in *IEEE Conf. on Robotics and Automation*, Albuquerque, Apr. 1997, pp. 193–198.
- [5] Q. Wang, Y. Huang, J. Zhu, B. Chen, and L. Wang, "Dynamic walking on uneven terrains with passivity-based bipedal robot," vol. 85, no. 3, pp. 187–199, 2011.
- [6] Z. Qiu-Bo, P. Song-Hao, and G. Chao, "Motion planning for humanoid robot based on hybrid evolutionary algorithm," vol. 7, no. 3, pp. 209–216, 2010.
- [7] P. Brugger and H. B. Schmedmayer, "Simulating prosthetic gait - lessons to learn," vol. 3, no. 1, p. 64, 2003.
- [8] J. K. Rai, R. P. Tewari, and D. Chandra, "Hybrid control strategy for robotic leg prosthesis using artificial gait synthesis," vol. 1, no. 1, pp. 44–50, 2009.
- [9] K. M. Ono, Kyosuke, "Analytical study of active prosthetic legs," vol. 1, no. 3, pp. 548–557, Mar. 2007.
- [10] H. Kazerooni, J. L. Racine, L. Huang, and R. Steger, "the control of the berkeley lower extremity exoskeleton," in *Proceedings of the 2005 IEEE International Conference on Robotics and Automation*, Barcelona, Apr. 2005, pp. 4353 – 4360.
- [11] J. Rose and J. G. Gamble, *Human Walking*. Philadelphia: Lippincott Williams & Wilkins, Dec. 2005.
- [12] A. D. Ames, "First steps toward automatically generating bipedal robotic walking from human data," in *8th International Workshop on Robotic Motion and Control, RoMoCo'11*, Bukowy Dworek, 2011.
- [13] Y. Xiang, J. Arora, H.-J. Chung, H.-J. Kwon, S. Rahmatalla, R. Bhatt, and K. Abdel-Malek, "Predictive simulation of human walking transitions using an optimization formulation," *Structural and Multidisciplinary Optimization*, pp. 1–14, Sep. 2011.
- [14] S. Jiang, S. Patrick, H. Zhao, and A. D. Ames, "Outputs of human walking for bipedal robotic controller design," in *2012 American Control Conference*, Montréal, Jun. 2012.
- [15] R. W. Sinnet, M. J. Powell, S. Jiang, and A. D. Ames, "Compass gait revisited: A human data perspective with extensions to three dimensions," in *50th IEEE Conference on Decision and Control and European Control Conference*, Orlando, Dec. 2011.
- [16] J. W. Grizzle, G. Abba, and F. Plestan, "Asymptotically stable walking for biped robots: Analysis via systems with impulse effects," *IEEE TAC*, vol. 46, no. 1, pp. 51–64, Jan. 2001.
- [17] Y. Hürmüzlü and D. B. Marghitu, "Rigid body collisions of planar kinematic chains with multiple contact points," *Intl. J. of Robotics Research*, vol. 13, no. 1, pp. 82–92, Feb. 1994.
- [18] R. M. Murray, Z. Li, and S. S. Sastry, *A Mathematical Introduction to Robotic Manipulation*. Boca Raton: CRC Press, Mar. 1994.
- [19] S. S. Sastry, *Nonlinear Systems: Analysis, Stability and Control*. New York: Springer, Jun. 1999.
- [20] A. D. Ames, "First steps toward underactuated human-inspired bipedal robotic walking," in *IEEE International Conference on Robotics and Automation*, St. Paul, May 2012.
- [21] A. D. Ames, E. A. Cousineau, and M. J. Powell, "Dynamically stable robotic walking with nao via human-inspired hybrid zero dynamics," in *Hybrid Systems: Computation and Control*, Beijing, Apr. 2012.